BMC Microbiology

RESEARCH

Open Access

Circadian rhythm perturbation causes IBS-like characteristics and altered fecal metabolome in mice

Gaichao Hong[1,2†], Yajuan Zhao[3†], Jieru Zhou[1], Lilin Hu[1], Gangping Li[1*] and Yu Jin[1*]

Abstract

Background Circadian rhythm disturbance is associated with functional gastrointestinal disorders such as irritable bowel syndrome (IBS). This study aimed to explore the effects of dysregulated circadian rhythm on visceral sensitivity, colonic permeability, gut microbial composition, and metabolism in mice.

Methods A murine model of circadian rhythm disturbance was built by performing a 6-hour phase delay. Visceral sensitivity was assessed using the abdominal withdrawal reflex score through colorectal distention. Colonic permeability was determined by measuring transepithelial resistance (TEER) and the permeability of fluorescent dextran 4 kDa. To gain insight into gut microbial composition and metabolism, 16S rRNA sequencing and untargeted metabolomics were conducted, respectively.

Results Circadian rhythm disturbance led to IBS-like characteristics in mice, including visceral hypersensitivity and colonic hyperpermeability. Disrupted circadian rhythm also resulted in a decrease in intestinal microbial diversity and alterations in microbial structure. Several microbial genera were influenced by circadian rhythm disturbance, such as *Bacteroides*, *Bifidobacterium*, *Desulfovibrio*, *Dubosiella,* and *Erysipelatoclostridium*. Moreover, disrupted circadian rhythm altered metabolic profiles of gut microbiota and affected the levels of various metabolites, including 1-methylhistamine, nitrosylhaem, 3-aminocaproic acid, boviquinone, and carboplatin. Finally, circadian rhythm disturbance altered the relationship between microbial genera and metabolites.

Conclusion Circadian rhythm disturbance contributes to visceral hypersensitivity and colonic hyperpermeability, while also altering the composition and metabolism of gut microbiota.

Keywords Circadian rhythm disturbance, Phase shift, IBS, Gut microbiota, Metabolism

Background

Irritable bowel syndrome (IBS) is a prevalent functional gastrointestinal disorder which manifests abdominal pain and altered stool frequency or form [1]. IBS is characterized by altered gut motility, intestinal mucosal hyperpermeability, and visceral hypersensitivity [2]. The global prevalence of IBS ranges from 10% to 20%. The condition is more prevalent in individuals with a history of acute intestinal infections and psychological comorbidities [3]. Although the pathophysiology of IBS remains incompletely elucidated, current evidence suggests that impaired gut barrier function, genetic factors, gut

†Gaichao Hong and Yajuan Zhao contributed equally to this work.

*Correspondence:
Gangping Li
ligangping@hust.edu.cn
Yu Jin
jinjoey@hust.edu.cn
[1] Division of Gastroenterology, Union Hospital, Tongji Medical College, Huazhong University of Science and Technology, Wuhan 430022, China
[2] Department of Gastroenterology, The First Affiliated Hospital of Guangzhou Medical University, Guangzhou, Guangdong, China
[3] Department of Gastroenterology, The Second Affiliated Hospital of Guangzhou Medical University, Guangzhou, Guangdong 510260, China

dysbiosis, immune dysregulation, and disordered brain-gut axis contribute to its development [4].

Circadian rhythms are endogenous cycles with a periodicity of ~24 hours that are present in mammals, organs, and cells. These rhythms are regulated by a light-entrainable clock, which mainly lies in the hypothalamic suprachiasmatic nucleus, but is also found in various tissues such as the liver, intestine, and adipose tissue [5]. To maintain body homeostasis, circadian rhythms need to synchronize with external cyclic signals, such as the 24-hour light-dark cycle. Disturbances in circadian rhythms have detrimental effects on physiology and immunity, contributing to metabolic disorders, gastrointestinal dysfunction, psychiatric syndrome, and cancer [6]. Shift work or work outside from 9 a.m. to 5 p.m. often leads to dysregulated circadian rhythms, which can aggravate IBS-associated symptoms, including constipation, diarrhea, bloating, gas, and abdominal pain [7]. A growing number of studies have revealed a strong association between shift work and IBS [8, 9].

Trillions of microbes inhabit the human intestine, forming a complex ecological community that influences physiology and susceptibility to disease [10]. Both IBS patients and animal models exhibit distinct microbial compositions compared with healthy individuals and control animals [11, 12]. Moreover, gut microbial dysbiosis can induce IBS-related symptoms in mice, such as visceral hypersensitivity and intestinal hyperpermeability [13]. These findings underscore the crucial role of gut microbiota in the pathophysiology of IBS. Altered circadian rhythm is also strongly associated with IBS, but further research is needed to elucidate the effect of circadian rhythm on gut microbial composition and microbial metabolites in IBS.

In order to disclose the impact of circadian rhythm disturbance on IBS-related characteristics and gut microbiota, we constructed a murine model using a 6-hour phase delay. By assessing visceral sensitivity and colonic permeability, as well as analyzing the composition of gut microbiota and metabolites, this study aimed to provide deep insights into the relationship among circadian rhythm dysregulation, IBS, and gut microbiota.

Methods

Animal experiment

Seven-week-old healthy male C57BL/6 J mice weighing 20–25 g purchased from Beijing Vital River Laboratory Animal Technology were fed in a specific-pathogen-free environment at the experimental animal center of Tongji Medical College, Huazhong University of Science and Technology. Mice were administered standard diets and water ad libitum at a temperature of 22℃ and 60% humidity. Fourteen healthy mice with similar weight and age were randomly divided into two groups: non-phase shift (NN; $n = 7$) and phase shift (PN; $n = 7$).

Mice in the NN group were housed in a light environment from 8:00 to 20:00 and kept in dark conditions from 20:00 to 8:00 (+1) for eight weeks. Mice in the PN group were subjected to light/dark phase shift through a 6-hour phase delay, and the detailed lightning schedules were as follows: light environment from 8:00 to 20:00 and dark condition from 20:00 to 8:00 (+1) during weeks 1 and 5; light environment from 8:00 to 14:00 and from 2:00 to 8:00 (+1), and dark condition from 14:00 to 2:00 during weeks 2, 4, 6, and 8; dark environment from 8:00 to 20:00 and light condition from 20:00 to 8:00 (+1) during weeks 3 and 7 [14]. The lighting schedules for both groups are shown in Fig. 1A.

At the end of the eighth week, visceral sensitivity was assessed, after which mice were anaesthetized to collect colonic samples. Specifically, euthanasia was performed by administrating 150 mg/kg sodium pentobarbital intraperitoneally. After confirming the absence of reflexes and cessation of breathing, mice were placed in dorsal recumbency, and the abdomen was disinfected using 70% ethanol. The abdominal cavity of the mouse was opened via a midline incision from the pubic symphysis to the xiphoid process. Next, the intestine was carefully retracted to expose the colon, and the distal colon near the rectum was ligated and transected distally. Finally, the ileocecal junction was identified and excised to isolate the colon, which was put into ice-cold physiological saline for evaluating colonic mucosal permeability. The animal experiment protocol was approved by the Animal Experiment Ethics Committee of Tongji Medical College, Huazhong University of Science and Technology.

Detection of visceral sensitivity

Abdominal withdrawal reflex (AWR) score was used to evaluate visceral sensitivity, which was determined as described below. A soft catheter equipped with an airbag was put into the colon at a depth of 1 cm via the anus of a fixed mouse, with the tail bound to the catheter. A three-way tube adaptor connected the catheter to a syringe and a pressure gauge. After a 20-minute acclimation period, colorectal distention was performed by pumping gas into the airbag at the pressure of 20, 40, 60, and 80 mmHg, each for a duration of 20 seconds, with a 5-minutes interval between inflations. The AWR score under each specific pressure was determined according to previously established standards [15].

Determination of colonic mucosal permeability

Colonic mucosal permeability was evaluated using transepithelial resistance (TEER, Ω·cm2) and fluorescent dextran 4 kDa (FD4) permeability (ng/mL/cm2/min)

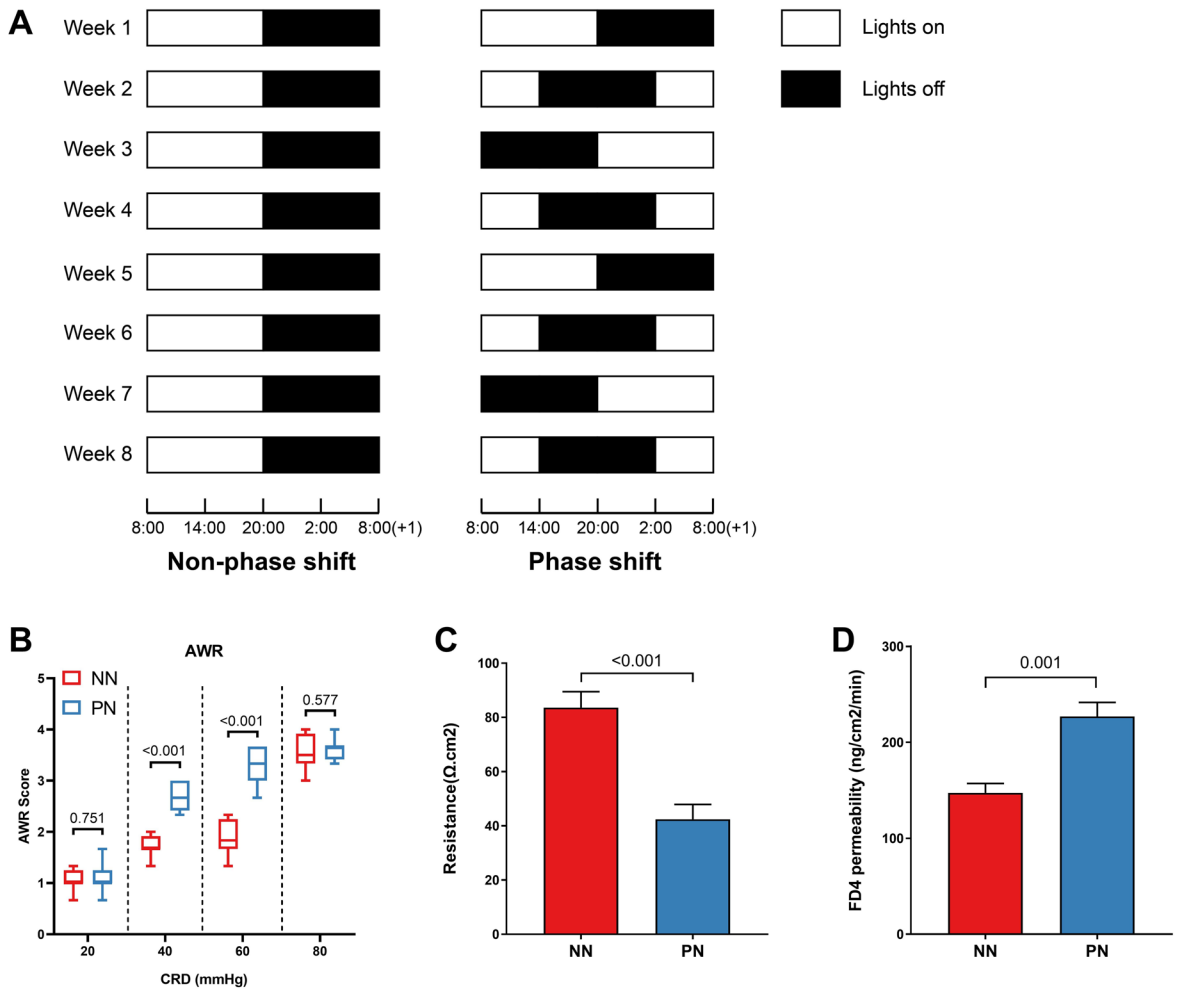

Fig. 1 Light/dark phase shift induced visceral hypersensitivity and colonic hyperpermeability. **A** The lighting schedules for NN and PN group. **B** Abdominal withdrawal reflex scores under different pressures of colorectal distension in NN and PN group. **C** Transepithelial resistance of colonic mucosa in NN and PN group. **D** Permeability to FITC-dextran of 4kD of colonic mucosa in NN and PN group. NN, Non-phase shift; PN, light/dark phase shift

[16]. In brief, a 1 cm segment of the colon was isolated from the mice, and the luminal surface was exposed. Then, the segment was placed into a Ussing chamber (Santiago, CA, USA), which was filled with Kreb's solution and infused with a gas mixture of 5% CO2 and 95% O2. After equilibration for 20 minutes, the TEER was measured by an automatic voltage clamp model. Subsequently, a solution containing 1 mg/mL fluorescein isothiocyanate-labeled FD4 was added to the mucosal side of the Ussing chamber. After 30 minutes, the solution on the serosal side was collected, and the intensity of FD4 in the solution was quantified using a Fluorescence Microplate Reader (Bio Tek, Winooski, VT, USA).

16S rRNA sequencing

Fecal samples were collected from mice for DNA extraction using the FastDNA SPIN Kit (Tiangen, Beijing, China). Fecal DNA concentration was detected by the Multiskan™ GO Fluorometer. The V3-V4 regions of the 16S rDNA were amplified using the 341 F and 806R primers. The ends of the 16S rDNA amplicons were linked with indexed adapters to construct indexed DNA libraries, whose concentration was quantified using Qubit 3.0 Fluorometer. The integrity of the DNA segments within the indexed libraries was assessed using Agilent 2100. Eligible DNA libraries were loaded into an Illumina high-throughput sequencing platform (Illumina, San Diego, CA, USA) to conduct paired-end sequencing. Raw reads

from the sequencing platform were combined and filtered using Flash to generate clean reads, from which chimeras were eliminated. The remaining reads were clustered into operational taxonomic units (OTUs) by Qiime [17], and OTUs were assigned taxonomically based on the Greengene database. Alpha diversity was assessed using Simpson, while beta diversity was evaluated using unweighted unifrac, which was visualized using principal coordinate analysis (PCoA) plot and tested using Adonis.

Untargeted metabolomics analysis

A 25 mg fecal sample was mixed with 500 µl of an extract solution consisting of acetonitrile, methanol, and water in a ratio of 2:2:1, along with an isotopically-labelled internal standard mixture. These samples were homogenized at 35 Hz for 4 minutes and sonicated for 5 minutes in an ice-water bath, and this process was repeated three times. After incubation at −40 ℃ for an hour, homogenized samples were centrifuged to extract supernatant. The quality control sample was produced by mixing equal aliquots of supernatants from all samples.

Liquid chromatography-tandem mass spectrometry (LC-MS/MS) analysis was performed using an ultra-high-performance liquid chromatography (UHPLC) system (Vanquish, Thermo Fisher Scientific) with a UPLC BEH Amide column coupled to a Q Exactive HFX mass spectrometer (Orbitrap MS, Thermo). The mobile phase consisted of 25 mmol/L ammonium acetate and 25 ammonia hydroxides in water (pH = 9.75) (A) and acetonitrile (B). The elution gradient in the mobile phase is listed in Table S1. The temperature of the column and auto-sampler was 30 ℃ and 4 ℃, respectively, and the injection volume was 3 µL.

The Q Exactive HFX mass spectrometer was used to acquire MS/MS spectra in information-dependent acquisition mode, controlled by the Xcalibur software (Thermo). In this mode, Xcalibur continuously evaluated the full scan MS spectrum. The ESI source conditions were set as follows: sheath gas flow rate at 50 Arb, Aux gas flow rate at 10 Arb, capillary temperature at 320 ℃, full MS resolution at 60000, MS/MS resolution at 7500, collision energy at 10/30/60 in NCE mode, and spray Voltage at 3.5 kV (positive) or −3.2 kV (negative), respectively.

The raw data were converted into mzXML format using ProteoWizard and processed with XCMS for peak detection, extraction, alignment, and integration. The metabolite annotation was performed using an in-house database called BiotreeDB. Differential metabolites between the two groups were identified using orthogonal partial least-square discriminant analysis (OPLS-DA), with selection criteria of variables importance in projection (VIP) > 1 and |log2 Foldchange| > 1. Differential metabolites were then clustered into metabolic pathways based on KEGG pathway enrichment using MetaboAnalyst 5.0 [18].

Statistical analysis

All the data were displayed as mean ± standard deviation. Unless otherwise stated, Student's t-test was used to compare two groups. Data was visualized using GraphPad Prism 8.0 and the ggplot2 package in R. Statistical analysis was performed using SPSS 22.0. Correlation analysis was performed using Spearman's rank correlation test. $P < 0.05$ was considered as statistical significance.

Results

Light/dark phase shift induced visceral hypersensitivity and colonic hyperpermeability

At colorectal distension pressures of 20 and 80 mmHg, the AWR score did not differ between the NN and PN groups (p=0.751 and p=0.577, Fig. 1B). However, the PN group exhibited higher AWR scores than the NN group at the pressures of 40 and 60 mmHg (p<0.001 and p<0.001, Fig. 1B), indicating that the Light/dark phase shift resulted in visceral hypersensitivity in mice. Additionally, the PN group had decreased transepithelial resistance of colon mucosa (p<0.001, Fig. 1C) and increased FD4 permeability (p=0.001, Fig. 1D) compared with the NN group, demonstrating that phase shift led to colonic mucosal hyperpermeability.

Light/dark phase shift altered gut microbial profiles

Gut microbiota was investigated in the NN and PN groups. As a result, we found that the Simpson index was decreased in the PN group compared with the NN group (p=0.032, Fig. 2A), and there was a clear separation between the NN and PN groups in the PCoA plot (p=0.038, Fig. 2B), indicating that phase shift reduced gut microbial diversity and impacted microbial structure. Moreover, no significant differences were observed in the predominant phyla between the NN and PN groups, including *Bacteroidetes* (p=0.81, Fig. 3B), *Firmicutes* (p=0.65, Fig. 3C), *Actinobacteria* (p=0.12, Fig. 3D), and *Proteobacteria* (p=0.81, Fig. 3E).

The composition of microbial genera was also influenced by phase shift. Specifically, the PN group showed a significantly decreased abundance of *Bacteroides* (p=0.012, Fig. 3G), *Candidatus Arthromitus* (p=0.04, Fig. 3H), *Parabacteroides* (p=0.026, Fig. 3I), *Muribaculum* (p=0.0089, Fig. 3J), *Erysipelatoclostridium* (p=0.0099, Fig. 3K), *Lactococcus* (p=0.024, Fig. 3L), and *Faecalibaculum* (p=0.02, Fig. 3M) compared with the NN group. Additionally, the abundance of some genera was significantly increased in the PN group compared with the NN group, including *Bifidobacterium* (p=0.0032,

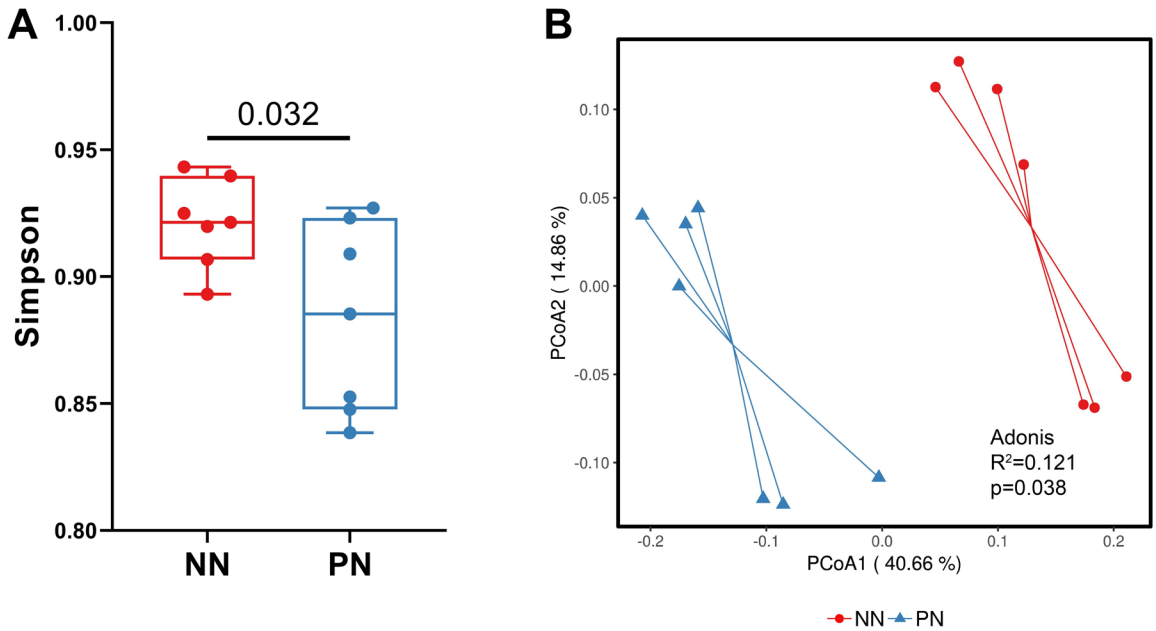

Fig. 2 Light/dark phase shift altered gut microbial structure. **A** Comparison of the Simpson index between NN and PN. **B** The PCoA plot showed gut microbial structure of NN and PN. Adonis was used to test statistical significance of PCoA. NN, Non-phase shift; PN, light/dark phase shift

Fig. 3N), *Desulfovibrio* (p=0.032, Fig. 3O), *Lachnospiraceae_FCS020_group* (p=0.018, Fig. 3P), *Dubosiella* (p=0.038, Fig. 3Q), *Prevotella_9* (p=0.03, Fig. 3R), *Ruminiclostridium_1* (p=0.013, Fig. 3S), *Ruminococcaceae_UCG_005* (p=0.026, Fig. 3T), and *Ruminococcaceae_UCG_010* (p=0.023, Fig. 3U). In summary, light/dark phase shift induced disturbance of gut microbiota in mice.

Light/dark phase shift disturbed the metabolism of gut microbiota

The metabolic profiles of NN and PN were visualized using OPLS-DA, which revealed a clear separation in metabolic structure between the NN and PN groups in both positive (Fig. 4A) and negative (Fig. 4B) modes. In the positive mode, 74 increased metabolites and 46 decreased metabolites were identified in the PN group compared with the NN group (Fig. 5A). Additionally, in the negative mode, PN exhibited 25 increased metabolites and 21 decreased metabolites compared with the NN group. Metabolites with a VIP > 2 and |log2 Fold-change| > 2 are shown in Fig. 6.

In the positive mode, 1−methylhistamine and nitrosylhaem were decreased in the PN group compared with the NN group. Additionally, 25 increased metabolites were found in the PN group, including 3-aminocaproic acid, carboplatin, GDP-D-mannurote, hydroxypyruvate, and D-Glycerate (Fig. 6A). In the negative mode, the PN group showed reduced abundances of coenzyme F420-1 and thyrotropin-releasing hormone compared with the NN group (Fig. 6B). The PN group had higher levels of specific metabolites than the NN group, such as chlomethoxyfen, flavonol 3-O-(6-O-malonyl-beta-D-glucoside), gallagic acid, termilin, 1-Methoxy-1H-indole-3-carboxaldehyde and urocanic acid (Fig. 6B).

Differential metabolites identified in the positive and negative modes were used for KEGG enrichment analysis, and several significantly enriched pathways were found. In the positive mode, significant pathways contained histidine metabolism, sphingolipid metabolism, vitamin B6 metabolism, arginine and proline metabolism, and pyrimidine metabolism (Fig. 7A). In the negative mode, there were five significantly different pathways between the NN and PN groups, including arachidonic acid metabolism, histidine metabolism, amino sugar and nucleotide sugar metabolism, pyrimidine metabolism, and tyrosine metabolism (Fig .7B).

Correlation analysis between gut microbiota and fecal metabolites in PN

To explore the potential association between gut microbiota and fecal metabolites in PN, Spearman correlation analyses were performed using genera and metabolites that were significantly different between the NN and PN group. Overall, we found 16 significantly positive and 40 significantly negative correlations in the PN group using differential metabolites in the positive mode and differential genera (Fig. 8A). Specifically, *Faecalibaculum*

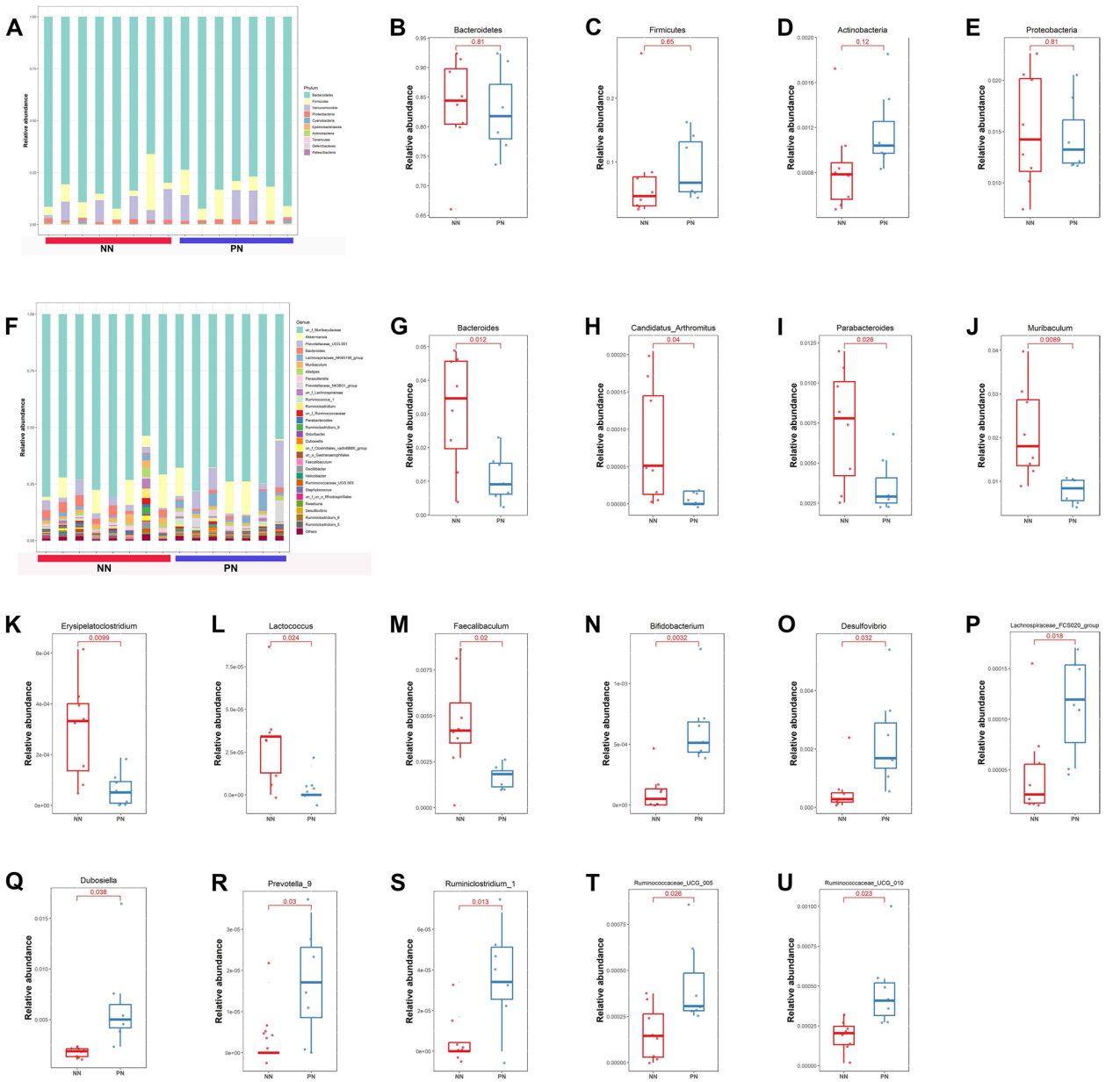

Fig. 3 Light/dark phase shift impacted gut microbial composition. **A** Distribution of microbial phyla in NN and PN. Comparison of predominant phyla between NN and PN, including (**B**) *Bacteroidetes*, **C** *Firmicutes*, **D** *Actinobacteria* and (**E**) *Proteobacteria*. (**F**) Distribution of microbial genera in NN and PN. **G**-**U** Comparison of different genera between NN and PN. NN, Non-phase shift; PN, light/dark phase shift

was positively correlated with two types of phosphatidylcholines, while *Prevotella_9* had positive correlations with carboplatin, glyphosate, and thymine. In contrast, *Bifidobacterium* was negatively associated with dTDP-4-dehydro-beta-L-rhamnose, palmitoleoyl ethanolamide, tazobactam, and trans-nochlor. *Erysipelatoclostridium* exhibited negative relationships with 1-methylhistamine, 5-amino-4-imidazole carboxylate, bowdichione, calcium glycerophosphate, capsiamide, diferuloylputrescine, dipropyl sulfide, isosorbide dinitrate, N-adenylylanthranilate, octadecanamide, and schidigeragenin C.

Furthermore, we identified 11 significantly positive and 22 significantly negative correlations in PN using differential metabolites in the negative mode (Fig. 8B). *Muribaculum* and *Ruminococcaceae_UCG_010* showed positive correlations with prostaglandin E3, while *Parabacteroides* and *Dubosiella* were positively correlated with primisulfuron. Conversely,

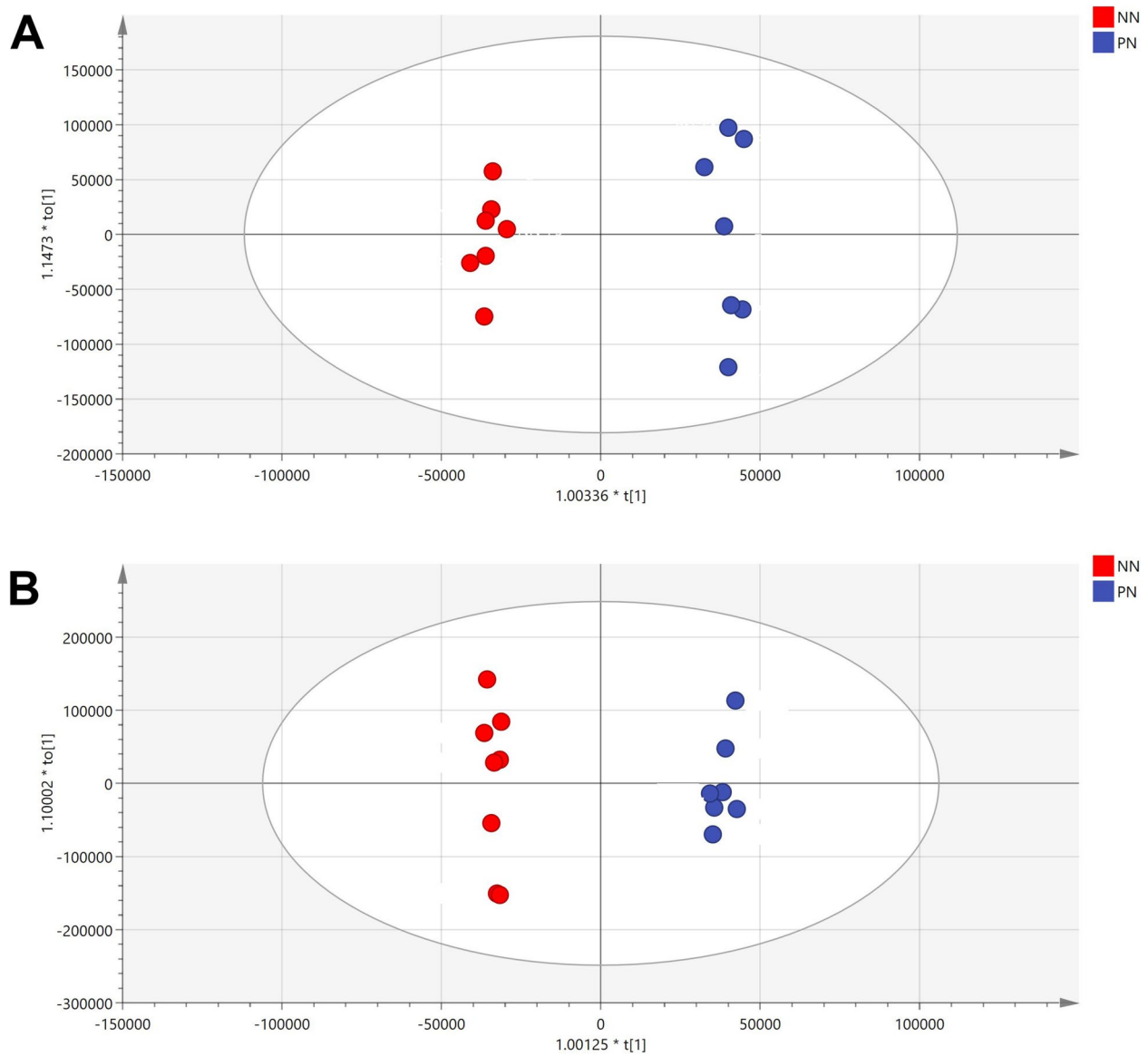

Fig. 4 Light/dark phase shift affected metabolic structure of gut microbiota. OPLS-DA score plots showed fecal metabolic structure of NN and PN in the (**A**) positive and (**B**) negative modes of untargeted metabolomics analysis. NN, Non-phase shift; PN, light/dark phase shift

Faecalibaculum was negatively associated with 2-ethyl-2-hydroxybutyric acid, 2-ketohexanoic acid, phenyllactic acid, and succinic acid. *Muribaculum* was negatively correlated with 4'-O-demethylrebeccamycin, hydroxymalote, and pyridoxine.

However, differential genera or metabolites between the NN and PN groups had no significant correlation with AWR scores, transepithelial resistance, and FD4 permeability of the colon in mice (Supplementary figure 1). In summary, there were strong associations between gut microbiota and fecal metabolites in PN.

Discussion

IBS is strongly associated with dysregulated circadian rhythm in the central nervous system and peripheral organs [19]. Previous studies have also indicated that altered circadian rhythm can disrupt gut microbiota. However, the complex interaction among altered circadian rhythm, IBS, gut microbiome, and microbial metabolites remains incompletely understood. In this study, a murine model of light/dark phase shift was constructed to investigate the impact of circadian rhythm disturbance on visceral sensitivity, colonic mucosal permeability, and

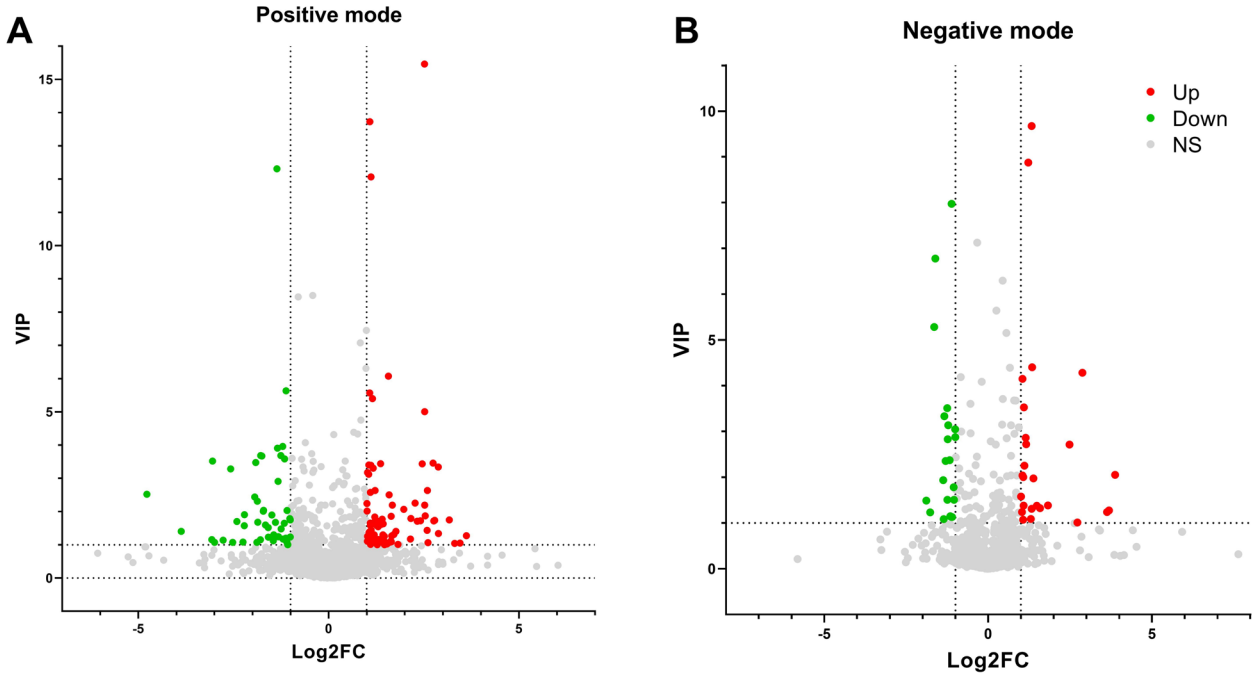

Fig. 5 Light/dark phase shift disturbed metabolism of gut microbiota. Volcano plots showed differential metabolites between NN and PN in the (**A**) positive and (**B**) negative modes of untargeted metabolomics analysis. Red and green dots represent upregulated and downregulated metabolites in PN compared with NN, respectively. NN, Non-phase shift; PN, light/dark phase shift

the composition and metabolites of gut microbiota. Our findings revealed that light/dark phase shift led to visceral hypersensitivity, colonic hyperpermeability, and significant alterations in gut microbial composition and metabolism. Our results provide important insights into the relationship between circadian rhythm, IBS, and gut microbiota.

Sleep disturbance [20] and shift work [8] have been strongly associated with functional gastrointestinal disorders. Individuals experiencing shift work and jet lag are reported to be more susceptible to gastrointestinal symptoms, such as abdominal pain, diarrhea, and constipation [21]. IBS patients with sleep disturbance have increased symptom severity scores compared with those without sleep disturbance, reinforcing evidence on the link between altered circadian rhythm and IBS [22]. Consistent with previous clinical studies, our animal experiment demonstrated that mice undergoing light/dark phase shift exhibited IBS-related characteristics, including visceral hypersensitivity and increased colonic permeability, which directly indicates that circadian rhythm disruption can lead to IBS symptoms.

This study found that light/dark phase shift could increase the abundance of *Desulfovibrio*, a H2S-producing bacteria enriched in diarrhea-predominant IBS (IBS-D) [23]. A murine model of IBS-D exhibited a distinct ileal microbiome profile characterized by an increased abundance of *Desulfovibrio* and elevated expression of genes associated with visceral hypersensitivity, including *Postn* and *Egfr* [24]. Furthermore, the administration of *Desulfovibrio* resulted in diarrhea-like phenotype in rats [25]. These findings suggest that IBS-related characteristics in PN mice is likely due to elevated level of *Desulfovibrio* in the intestine.

Light/dark phase shift also increased the abundance of *Dubosiella*, *Prevotella,* and *Ruminiclostridium*, which were recognized to produce butyrate [26, 27]. Compared with healthy controls, patients with IBS-D showed increased levels of butyrate [28], which positively correlated with the severity of IBS symptoms [29]. The murine model of IBS-D also presented a higher level of butyrate than control mice. Butyrate can promote the rate of colonic transit by facilitating the secretion of 5-HT [30]. These results suggest that increased levels of butyrate-producing bacteria might cause IBS-related characteristics in PN mice in our study.

Some studies demonstrated that IBS patients exhibit altered gut microbiota metabolic pathways compared with healthy individuals, including short-chain fatty acid, tryptophan, and bile acid metabolism [31]. In animal experiments, *Lactobacillus murinus*-derived spermidine was proven to directly trigger visceral hypersensitivity

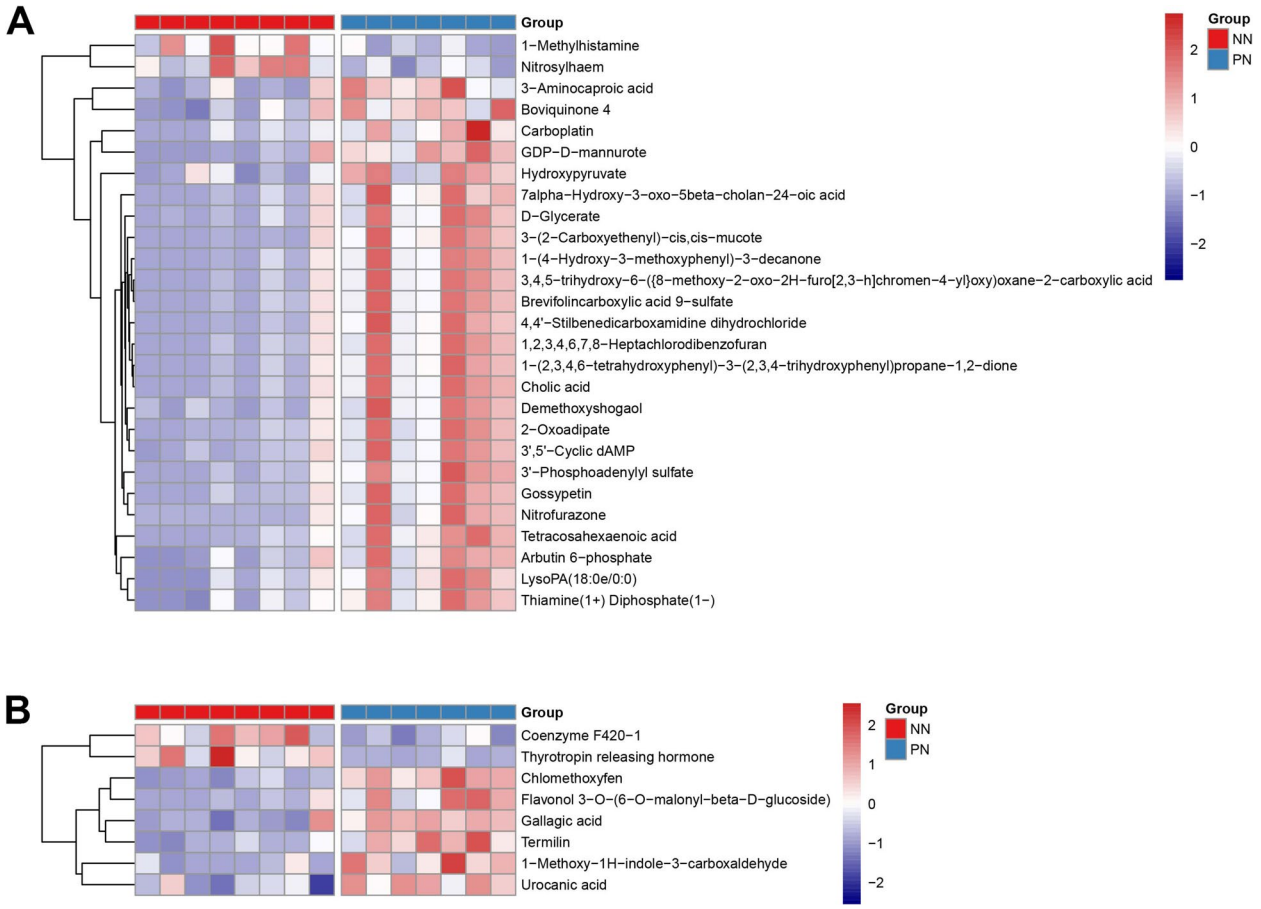

Fig. 6 Light/dark phase shift influenced levels of some microbial metabolites. Heatmaps showed relative concentrations of differential metabolites between NN and PN in the (**A**) positive and (**B**) negative modes of untargeted metabolomics analysis. T-test was used to compare metabolites of NN and PN. NN, Non-phase shift; PN, light/dark phase shift

[32], while *Ruminococcus gnavus*-produced phenethylamine and tryptamine were found to stimulate serotonin biosynthesis in intestinal enterochromaffin cells to promote gastrointestinal transit and colonic secretion [33]. These findings establish a connection between microbial metabolites and the pathophysiology of IBS.

In the present study, phase shift elicited an impact on several microbial metabolites and metabolic pathways, which might lead to IBS-like characteristics in mice. PN mice exhibited distinct gut microbial metabolic profiles compared with NN mice, with some differential metabolic pathways implicated in IBS, such as arachidonic acid and vitamin B6 metabolism. Dysregulation of arachidonic acid metabolism can lead to low-grade mucosal inflammation [34], which was observed in the colons of IBS patients and considered an underlying mechanism of IBS [35]. Additionally, low intake of vitamin B6 correlated with high IBS symptom scores [36], and abdominal symptoms in IBS patients were alleviated by vitamin B6 supplementation [37]. Therefore, alterations in arachidonic acid and vitamin B6 metabolism are likely to induce IBS-associated characteristics in PN mice.

The present study has several limitations. First, it does not uncover whether or how circadian rhythm disturbance influences intestinal mucosal microbiota, which plays an important role in the pathogenesis of IBS. Second, 16S rRNA sequencing does not provide information about the distribution of microbial species, warranting the need for shotgun metagenomics sequencing for a more comprehensive analysis. Lastly, fecal microbiota transplantation was not performed to determine the impact of altered microbiota and metabolites in PN mice on IBS-associated characteristics.

Conclusions

This study sheds light on the relationship between circadian rhythm disturbance and IBS-associated characteristics, as well as the composition and metabolism of gut

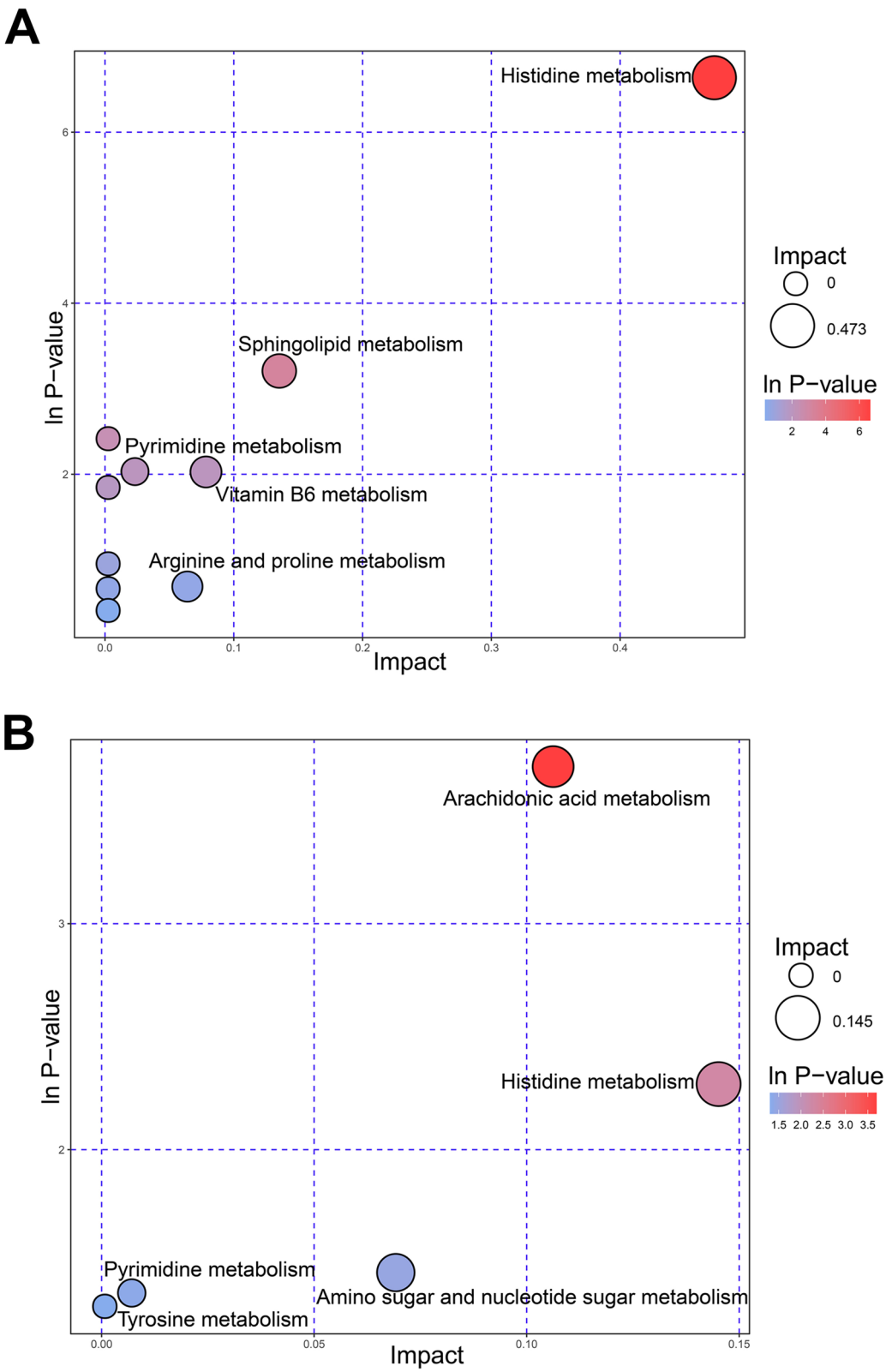

Fig. 7 Light/dark phase shift altered metabolic pathways of gut microbiota. Remarkably differential KEGG pathways between NN and PN in the (**A**) positive and (**B**) negative modes of untargeted metabolomics analysis

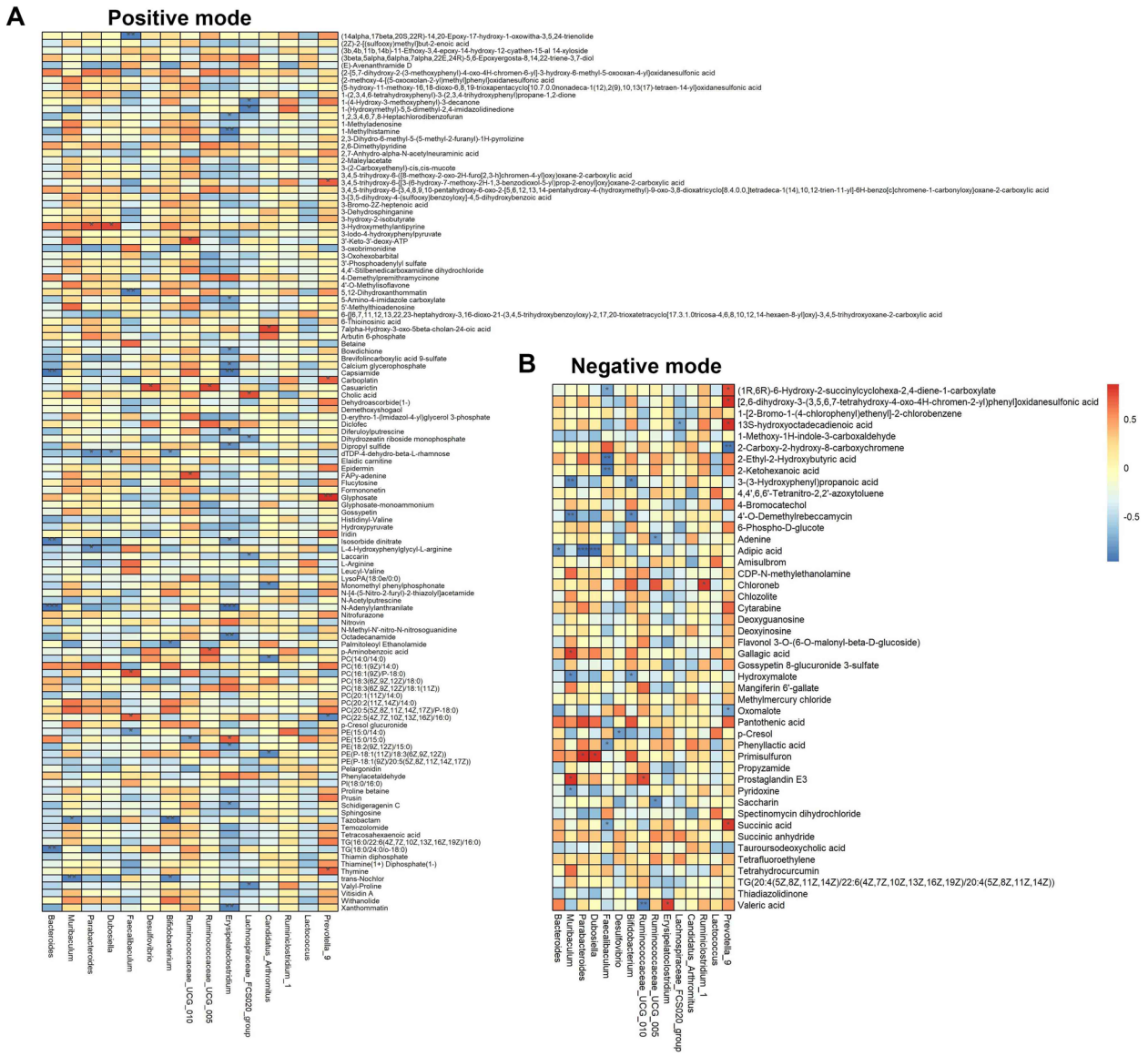

Fig. 8 Correlation analysis between gut microbiota and fecal metabolites in PN. Spearman correlations between microbial genera and metabolites were performed in PN group in the (**A**) positive and (**B**) negative modes of untargeted metabolomics analysis. Differential genera and metabolites between NN and PN were used in correlation analysis. Asterisk means significant correlation

microbiota. These findings suggest that circadian rhythm disruption can induce IBS-like characteristics and lead to changes in gut microbial composition and metabolism. The study demonstrates that microbial dysbiosis may underlie the development of IBS-like symptoms caused by circadian rhythm disturbance, although further studies are needed to validate this hypothesis.

Abbreviations

AWR	Abdominal withdrawal reflex
CRD	Colorectal distension
TEER	Transepithelial resistance
FD4	FITC-dextran of 4kD
PCA	Principal Component Analysis
PCoA	Principal Co-ordinates Analysis
IBS	Irritable bowel syndrome
IBS-D	Diarrhea-predominant irritable bowel syndrome
NN	Non-phase shift
PN	Light/dark phase shift

Supplementary Information

The online version contains supplementary material available at https://doi.org/10.1186/s12866-025-04009-0.

Supplementary Material 1.

Supplementary Material 2.

Acknowledgements
Not applicable.

Authors' contributions
Gaichao Hong: Writing – original draft, Visualization, Validation, Supervision, Software, Resources, Methodology, Investigation, Formal analysis, Data curation, Conceptualization. Yajuan Zhao: Writing – review & editing, Validation, Supervision, Software. Jieru Zhou, Writing – review & editing. Lilin Hu, Writing – review & editing. Gangping Li, Writing – review & editing, Supervision, Conceptualization. Yu Jin: Writing – review & editing, Supervision, Funding acquisition, Conceptualization.

Funding
This study was supported by The Second Affiliated Hospital of Guangzhou Medical University (Nos.0803030055), Plan on Enhancing Scientific research in GMU (Nos. 2025SRP010) and Guangzhou Municipal Science and Technology Bureau (Nos. SL2024A04J01628).

Data availability
16S rRNA sequence data in this study are available in the Genome Sequence Archive (GSA) database (GSA accession number: PRJCA038177), which can be accessed at https://bigd.big.ac.cn/gsa/browse/CRA024397. Data from metabolomics were described in Table S2-S3.

Declarations

Ethics approval and consent to participate
The protocol of animal experiment was approved by the Animal Experimentation Ethics Committee of Tongji Medical College, Huazhong University of Science and Technology (Ethical approval number: S2659).

Consent for publication
All authors consent for publication of this manuscript.

Competing interests
The authors declare no competing interests.

Received: 31 October 2024 Accepted: 28 April 2025
Published online: 07 May 2025

References

1. Sultan S, Malhotra A. Irritable bowel syndrome. Ann Intern Med. 2017;166(11):ITC81–96.
2. Camilleri M, Boeckxstaens G. Irritable bowel syndrome: treatment based on pathophysiology and biomarkers. Gut. 2023;72(3):590–9.
3. Black CJ, Ford AC. Global burden of irritable bowel syndrome: trends, predictions and risk factors. Nat Rev Gastroenterol Hepatol. 2020;17(8):473–86.
4. Camilleri M, Dilmaghani S. Update on treatment of abdominal pain in irritable bowel syndrome: a narrative review. Pharmacol Ther. 2023;245:108400.
5. Hu L, et al. Circadian dysregulation induces alterations of visceral sensitivity and the gut microbiota in light/dark phase shift mice. Front Microbiol. 2022;13:935919.
6. Rijo-Ferreira F, Takahashi JS. Genomics of circadian rhythms in health and disease. Genome Med. 2019;11(1):82.
7. Duboc H, Coffin B, Siproudhis L. Disruption of circadian rhythms and gut motility: an overview of underlying mechanisms and associated pathologies. J Clin Gastroenterol. 2020;54(5):405–14.
8. Kim HI, et al. Impact of shiftwork on irritable bowel syndrome and functional dyspepsia. J Korean Med Sci. 2013;28(3):431–7.
9. Nojkov B, et al. The impact of rotating shift work on the prevalence of irritable bowel syndrome in nurses. Am J Gastroenterol. 2010;105(4):842–7.
10. Lynch SV, Pedersen O. The human intestinal microbiome in health and disease. N Engl J Med. 2016;375(24):2369–79.
11. Zhu X, et al. Understanding of the site-specific microbial patterns towards accurate identification for patients with diarrhea-predominant irritable bowel syndrome. Microbiol Spectr. 2021;9(3):e0125521.
12. Tao E, et al. Early life stress induces irritable bowel syndrome from childhood to adulthood in mice. Front Microbiol. 2023;14:1255525.
13. De Palma G, et al. Transplantation of fecal microbiota from patients with irritable bowel syndrome alters gut function and behavior in recipient mice. Sci Transl Med. 2017;9(379):eaaf6397.
14. Liu X, et al. Bidirectional regulation of circadian disturbance and inflammation in inflammatory bowel disease. Inflamm Bowel Dis. 2017;23(10):1741–51.
15. Jin Y, et al. Beneficial effects of Rifaximin in post-infectious irritable bowel syndrome mouse model beyond gut microbiota. J Gastroenterol Hepatol. 2018;33(2):443–52.
16. Zhang L, et al. EphrinB2/ephB2-mediated myenteric synaptic plasticity: mechanisms underlying the persistent muscle hypercontractility and pain in postinfectious IBS. FASEB J. 2019;33(12):13644–59.
17. Caporaso JG, et al. QIIME allows analysis of high-throughput community sequencing data. Nat Methods. 2010;7(5):335–6.
18. Pang Z, et al. MetaboAnalyst 5.0: narrowing the gap between raw spectra and functional insights. Nucleic Acids Res. 2021;49(W1):W388–96.
19. Heitmann PT, et al. Understanding the physiology of human defaecation and disorders of continence and evacuation. Nat Rev Gastroenterol Hepatol. 2021;18(11):751–69.
20. Koloski NA, et al. Sleep disturbances in the irritable bowel syndrome and functional dyspepsia are independent of psychological distress: a population-based study of 1322 Australians. Aliment Pharmacol Ther. 2021;54(5):627–36.
21. Knutsson A, Boggild H. Gastrointestinal disorders among shift workers. Scand J Work Environ Health. 2010;36(2):85–95.
22. Tu Q, et al. Sleep disturbances in irritable bowel syndrome: a systematic review. Neurogastroenterol Motil. 2017;29(3):e12946.
23. Villanueva-Millan MJ, et al. Methanogens and hydrogen sulfide producing bacteria guide distinct gut microbe profiles and irritable bowel syndrome subtypes. Am J Gastroenterol. 2022;117(12):2055–66.
24. Leite G, et al. Cytolethal distending toxin B inoculation leads to distinct gut microtypes and IBS-D-like microRNA-mediated gene expression changes in a rodent model. Gut Microbes. 2024;16(1):2293170.
25. Villanueva-Millan MJ, et al. Hydrogen sulfide producers drive a diarrhea-like phenotype and a methane producer drives a constipation-like phenotype in animal models. Dig Dis Sci. 2024;69(2):426–36.
26. Qiao S, et al. Gut Parabacteroides merdae protects against cardiovascular damage by enhancing branched-chain amino acid catabolism. Nat Metab. 2022;4(10):1271–86.
27. Huang J, et al. Ginseng polysaccharides alter the gut microbiota and kynurenine/tryptophan ratio, potentiating the antitumour effect of antiprogrammed cell death 1/programmed cell death ligand 1 (anti-PD-1/PD-L1) immunotherapy. Gut. 2022;71(4):734–45.
28. Gargari G, et al. Fecal Clostridiales distribution and short-chain fatty acids reflect bowel habits in irritable bowel syndrome. Environ Microbiol. 2018;20(9):3201–13.
29. Tana C, et al. Altered profiles of intestinal microbiota and organic acids may be the origin of symptoms in irritable bowel syndrome. Neurogastroenterol Motil. 2010;22(5):512–9, e114-5.
30. Shaidullov IF, et al. Short chain fatty acids and colon motility in a mouse model of irritable bowel syndrome. BMC Gastroenterol. 2021;21(1):37.
31. Mars RAT, et al. Longitudinal multi-omics reveals subset-specific mechanisms underlying irritable bowel syndrome. Cell. 2020;182(6):1460-1473 e17.
32. Zhang L, et al. Stress triggers irritable bowel syndrome with diarrhea through a spermidine-mediated decline in type I interferon. Cell Metab. 2025;37(1):87–103 e10.
33. Zhai L, et al. Ruminococcus gnavus plays a pathogenic role in diarrhea-predominant irritable bowel syndrome by increasing serotonin biosynthesis. Cell Host Microbe. 2023;31(1):33–44 e5.
34. Xu M, et al. Arachidonic acid metabolism controls macrophage alternative activation through regulating oxidative phosphorylation in PPAR-gamma dependent manner. Front Immunol. 2021;12:618501.
35. Cremon C, et al. Mucosal immune activation in irritable bowel syndrome: gender-dependence and association with digestive symptoms. Am J Gastroenterol. 2009;104(2):392–400.

36. Ligaarden SC, Farup PG. Low intake of vitamin B6 is associated with irritable bowel syndrome symptoms. Nutr Res. 2011;31(5):356–61.
37. Bonfrate L, et al. Effects of Bifidobacterium longum BB536 and Lactobacillus rhamnosus HN001 in IBS patients. Eur J Clin Invest. 2020;50(3):e13201.

Publisher's Note